This is a repository copy of *Mitotic quiescence, but not unique "stemness," marks the phenotype of bone metastasis-initiating cells in prostate cancer*.

White Rose Research Online URL for this paper:
http://eprints.whiterose.ac.uk/97674/

Version: Submitted Version

1   **Title:**

2   **Mitotic quiescence, but not unique 'stemness', marks the phenotype of bone metastasis initiating**

3   **cells in prostate cancer.**

4

5   **Ning Wang[1], Freyja Docherty[1], Hannah K Brown[1], Kim Reeves[3], Anne Fowles[1], Michelle Lawson[2],**

6   **Penelope D Ottewell[2], Ingunn Holen[2], Peter I Croucher[4], Colby L Eaton[1*].**

7

8   **Running title: Tumor cell quiescence in bone metastases**

9

10

11   **Affiliations:**

12   [1] Department of Human Metabolism, Medical School, University of Sheffield, UK

13   [2] Department of Oncology, Medical School, University of Sheffield, UK

14   [3] Break Through Breast Cancer Research Unit, Paterson Institute for Cancer Research Manchester, UK

15   [4] Bone Biology Division, Garvan Institute of Medical Research, Sydney, Australia

16

17

18   *** Corresponding author:**

19   Dr Colby L Eaton

20   Academic Unit of Bone Biology

21   Department of Human Metabolism

22   D Floor, The Medical School

23   Beech Hill Road

24   Sheffield

25   S10 2RX

26   UK

27   Telephone: 44 (0)114 226 1204

28   Fax: 44 (0)114 271 2475

29   Email: c.l.eaton@sheffield.ac.uk

30   The authors disclose no potential conflicts of interest.

31

Abstract

Purpose: this study aimed to identify subpopulations of prostate cancer cells that are responsible for the initiation of bone metastases.

Procedures: Using rapidly dividing human prostate cancer cell lines, we identified mitotically quiescent subpopulations (<1%), which we compared with the rapidly dividing populations for patterns of gene expression and for their ability to migrate to the skeletons of athymic mice. The study used 2-photon microscopy to track migration of fluorescently labeled cells and luciferase expression to determine the presence of growing bone metastases.

Findings: We showed that the mitotically quiescent cells were very significantly more tumourogenic in forming bone metastases than fast growing cells (55% vs 15%) and had a unique gene expression profile. The quiescent cells were not uniquely stem-cell like, with no expression of CD133 but same level expression of other putative prostate stem cell markers (CD44 and integrins $\alpha2/\beta1$), when compared to the rapidly proliferating population. In addition, mitotic quiescence was associated with very high levels of CXCR4 production. Inhibition of CXCR4 activity altered the homing of quiescent tumour cells to bone.

Conclusions: Mitotic dormancy is a unique phenotype that facilitates tumour cell colonization of the skeleton in prostate cancer.

Introduction

Although prostatectomy is a successful treatment for prostate cancer that appears to be organ confined, in a significant number of patients the disease progresses, primarily by metastasis to the skeleton. In some cases this occurs many years after removal of the primary cancer so that it is clear that trafficking of tumor cells in/out of the bone microenvironment occurs at an early stage in the disease in some patients. It is also likely that this continues throughout the disease and is a major driver of disease progression.

Recent studies have suggested that prostate cancers contain stem cell-like populations (1-9) and these may contribute to tumor heterogeneity and their adaptability. Others have suggested disseminating prostate cancer cells locate to 'niches' within the bone marrow, normally occupied by haematopoietic stem cells (HSCs) (10). However, the phenotype of the metastasis initiating population remains elusive, although it is believed that metastasizing cells will be mitotically quiescent. In this state they could survive in specific metastatic niches and their lack of proliferation would allow them to remain undetected for extended periods of time and confer resistance to anti-proliferative agents.

We have studied several human prostate cancer cell lines in vitro to determine if they contain subpopulations that are mitotically quiescent with metastasis initiating potential. The cell lines were stained with vital lipophilic fluorescent dyes and followed in culture for several weeks. These dyes are very bright and importantly, are lost as cells divide, allowing non-dividing/slowly dividing cells, referred to here as quiescent, to be identified and distinguished from proliferating cells (11). Using this method we have isolated and characterized a low frequency, quiescent population from all cell lines. These cells or equivalent numbers of rapidly dividing cells were injected into the circulation of athymic mice and tumour growth assessed using bioluminescent in vivo imaging and post-mortem histology/2-photon microscopy. We assessed the relative capacities of these populations to form skeletal tumours in these animals. We have also presented a gene expression profile for quiescent cells.

Methods

Cell lines

The PC3 prostate cancer cell line (ATCC) was stably transfected with a firefly luciferase gene luc2 (pGL4.51 [luc2/CMV/Neo] vector, Promega) using a Gene Pulser^{TM} electroporator (Bio-Rad) (denoted PC3-NW1) and transfected with Amaxa pmaxGFP vector (Lonza) (PC3-GFP). LNCaP were purchased from ATCC (ATCC) and the C4 2B4 strain supplied by the University of Bern (Switzerland). All cell lines were maintained in Dulbecco's Modified Eagle's Medium (Gibco, Life Technologies), supplemented with

87 antibiotics and foetal bovine serum (Sigma Aldrich). All cell lines were genetically profiled by Stem Elite

88 ID system (Promega) that confirmed their identity (18/18 STRs).

89

90 **Mitotically quiescent cells in vitro**

91 **Defining the quiescent population in vitro**

92 Prostate cancer cells were stained in suspension with 5μM lipophilic carbocyanine dye Vybrant DiD (Life

93 Technologies) according to the manufacturers instructions. The proportion of cells retaining the dye

94 with/without a 3hr pretreatment of 5µg/mL Mitomycin C (Sigma Aldrich) were analyzed by FACS (Calibur

95 , BD Biosciences, Oxford, UK). Cells were imaged using a Leica DMI 4000B microscope (Leica

96 Microsystems GmbH). The effect of lipophilic dyes on cell proliferation was determined by quantifying

97 cell number up to 12 days in culture to determine the cell cycle phase of the quiescent population. DiD

98 labeled PC3-NW1 cells were seeded at 6000/cm2 into a Permanox® Lab-Tek® Chamber Slide System

99 (Thermo Scientific) and subcultured for 14 days. Mouse anti-human Ki-67 antibody (BD Bioscience) was

100 then used to identify the growing cells according to the manufacturer's protocol. The fraction of Ki-67

101 positive (Ki-67+) to negative (Ki-67-) cells were analyzed using the FACS Calibur flow cytometer and

102 compared between the DiD positive (DiD+) and negative (DiD-) populations.

103

104 **TaqMan® Custom Array**

105 Mitotically quiescent and rapidly dividing cells were isolated on day 14 by FACS and total RNA extracted

106 using the ReliaPrep™ RNA Cell Miniprep System (Promega). cDNA was synthesized using SuperScript™

107 III reverse trancriptase (Invitrogen, Life technologies) with a 1:1 mix of Oligo(dT) 15 and Random primers

108 (Promega) and samples analyzed using a 96 gene TaqMan® low density array (Applied Biosystems) with

109 an Applied Biosystems 7900HT Real-Time PCR system (Applied Biosystems) (50°C, 2min, 94.5°C, 10

110 min, 97.0°C, 30 s, 59.7°C, 1 min, repeated x40), covering markers of stem cells, HSC niche components,

111 epithelial to mesenchymal transition (EMT), extracellular matrix (ECM) and osteomimicry (complete list

112 in Supplementary tables 1 and 2). Data was analysed using the Applied Biosystems SDS 2.3 software.

113 Quantification of the target cDNAs in all samples was normalized to the endogenous control gene: GAPDH

114 ($\Delta CT = CT_{target} - CT_{GAPDH}$). The difference in expression for each target cDNA between the between

115 quiescent/non-quiescent cells was expressed as $\Delta\Delta CT$ ($\Delta\Delta CT = \Delta CT_{quiescent} - \Delta CT_{non-quiescent}$). The relative

116 expression levels (fold changes) were the calculated using 2 to the power of the $\Delta\Delta CT$ ($2^{-\Delta\Delta CT}$), a two-fold

117 expression change between cell types was deemed significant (Supplementary table 2).

118

119 **Immunofluorescence staining**

4

DiD labeled prostate cancer cells were subcultured for 14 days and cytospun onto slides. The cells were formalin fixed and stained with anti-human CXCR4 phycoerythrin conjugated monoclonal antibody (Clone 12G5) or mouse IgG2A isotype control (R&D Systems) (1h, 20°C). For intracellular staining of matrix metalloproteinase-3 (MMP3) (using mouse monoclonal anti-MMP3 antibody) and follistatin (using mouse monoclonal anti-follistatin antibody) (Abcam, Cambridge, UK), the formalin fixed cells were permeablised first in 0.5 % tween diluted in PBS (PBST) and incubated with primary antibodies or isotype controls overnight at 4°C, followed by 30 minutes incubation with Goat anti-mouse IgG secondary antibody (Alexa Fluor® 488)(Abcam). All samples were then counterstained with 4',6-Diamidino-2-phenylindole, dihydrochloride (DAPI) and imaged with a Leica AF6000 time lapse microscope (Leica Microsystems). The intensity of the immunofluorescence was then quantified with ImageJ software and compared between DiD+ and DiD- populations.

Mitotically quiescent cells in vivo

Mice

Male BALB/c nude immunocompromised mice (Charles River) were used and all procedures complied with the UK Animals (Scientific Procedures) Act 1986 (PPL 40/3462).

Intracardiac injection of tumor cells

PC3-NW1 cells were stained with 5μM DiD and single-cell suspensions of 1×10^5 DiD labeled PC-3 cells/100 μL PBS were injected into the left cardiac ventricle (intracardiac (i.c.) injection) of 6-week-old male BALB/c nude mice. Tumor growth was monitored for 6 weeks post injection using in vivo imaging systems (IVIS Caliper Life Sciences for detection of PC3-NW1 and the Illumatool Lighting System (LightTools Research) for detection of PC3-GFP). Cohorts of animals (n>6/group) were euthanized at different times post injection. DiD labeled LNCaP and C4 2B4 cells were also injected (i.c.) into 6-week-old male BALB/c nude mice and animals were euthanized at 7 days post injection to confirm the presence of quiescent tumour cells in bone microenvironment.

Multiphoton (2-Photon) microscopy

Dissected tibias were snap-frozen in liquid nitrogen, embedded in Cryo-M-Bed compound and trimmed longitudinally to expose bone marrow area using a cryostat (Bright Instrument Co. Ltd). A stack area of 2104μm x 2525μm below the growth plate with 100μm in depth was imaged (Zeiss LSM510 NLO two-photon microscope Carl Zeiss) and reconstructed with the LSM software 4.2 (Carl Zeiss Microscopy Ltd, Cambridge, UK) as previously described (12). A 633nm and 543nm HeNe laser was used to detect DiD and CM-DiI cells respectively. The bone and PC3-GFP cells were detected using the 900nm Chameleon

154 multiphoton laser (Coherent, Santa Clara, CA.). The quantitative data; tumor cell number, size and distance

155 from cell centroid to bone surface, were then analyzed by Volocity 3D Image Analysis software 6.01

156 (PerkinElmer).

157

158 **Disruption the CXCR4 signalling in vivo**

159 DiD labeled 1×10^5 PC3-NW1 cells were i.c injected into 6-week-old male BALB/c nude mice. Seven days

160 post injection, animals were subject to 5 days of treatment with CXCR4 inhibitor AMD3100 (5mg/kg, daily

161 intrperitoneal injection)(Sigma Aldrich Co. Ltd, Poole, UK) or with PBS control (Figure 3D). Animals

162 were then euthanized and the presence of DiD labelled tumour cells were examined and quantified using

163 two-photon microscopy in tibias ex vivo.

164

165 **Comparison of the tumor forming ability of the quiescent and non-quiescent subpopulations.**

166 PC3-NW1 cells were stained with 5μM DiD, subcultured and maintained at a density of at least 5×10^5

167 cells/cm^2 for 14 days. The DiD positive (DiD+) quiescent and negative (DiD-) fast growing subpopulations

168 sorted by FACS (Aria cell sorter BD Biosciences, Oxford, UK). DiD+ quiescent cells were injected (i.c.)

169 into 6-week-old male BALB/c nude mice (5×10^3 cells/mouse, n=15). DiD- non-quiescent cells were re-

170 stained with another lipophilic dye CellTracker, CM-DiI (Life Technologies) before injection (i.c) into age-

171 matched mice at two different concentrations (5×10^3 cells/mouse, n=15 and 1×10^5 cells/mouse, n=10), to

172 allow tracking by 2-photon microscopy. A control, unsorted population of PC3-NW1 cells was passed

173 through the FACS-Aria and 1×10^5 of these cells labeled with DiD and injected (i.c. n=10). Tumor growth

174 was monitored up to 6 weeks post injection (IVIS) and the tumour burden was evaluated using the Living

175 Imaging® In Vivo Imaging software (PerkinElmer Inc. Massachusetts, USA) based on photon radiance.

176 The presence of DiD+/CM-Dil+ cells was also determined in tibias using 2-Photon microscopy post-

177 mortem.

178

179 **Statistical analysis**

180 All data are expressed as mean ± SEM. Statistical significance was tested for using an unpaired Student's

181 t-test with or without Welsh's correction or one-way ANOVA with post hoc Tukey test as appropriate using

182 the Prism 6 software (GraphPad). P< 0.05 was considered to be significant.

183

184

185 **Results:**

186 **Prostate cancer cell lines contain mitotically quiescent cell populations at low frequencies.**

187 PC3-NW1, LNCap and C4 2B4 cells were stained with DiD and followed for up to 3 weeks by flow
188 cytometry. The proportion of cells labeled with DiD (% DiD+ve) did not change during the first 3 days,
189 but rapidly declined to a steady level of dye retention by day 14. At this and later time points, a dye retentive
190 population was present at a low frequency (<2%) (Figure 1 A, B, C). To test whether loss of dye was a
191 result of proliferation (Figure 1A), cell division was inhibited in some cultures by treatment with Mitomycin
192 C. This resulted in dye retention in a high percentage of cells. Cell proliferation under standard conditions
193 was unaffected by DiD treatment (Figure 1D).

194

195 To test the viability and proliferative potential of quiescent cells, cells that had retained DiD for 14 days in
196 standard cultures were isolated by FACS and re-cultured at clonal density. The cells attached to dishes
197 within 24h and remained as single cells for 3-5 days. After this time cells started to form colonies in which
198 dye was sequentially lost in most but not all cells. (Figure 1E). This suggests that DiD retaining populations
199 isolated by FACS remained viable and after a short delay, regained the ability to divide when cultured at
200 low density. The retention of dye by some cells and its loss in most (Figure 1E, Day 10) may suggest some
201 asymmetry in proliferation with some cells remaining relatively quiescent.

202

203 When DiD retaining cells and proliferating cells were separated by FACS, dye retaining cells showed
204 heterogeneity in proliferative marker Ki67 with both negative and positive staining within the population.
205 However, the percentage of cells that were Ki67 positive were significantly lower in the DiD retaining
206 population than in the proliferating cells (Figure 1 F,G).

207

208 **Mitotically quiescent populations have a distinctive gene expression profile**
209 The Taqman custom arrays defined clear and significant differences in the genes expressed by quiescent
210 (dye retaining) and non-quiescent populations isolated by FACS. In particular, type 1 collagen, CXCR4,
211 fibronectin, follistatin, matrilin 2, MMP 2 and 3, prostate stem cell antigen, TMPRSS2, tenascin 3 and
212 vitronectin were expressed at >2.5 fold higher levels in the quiescent population compared to the non-
213 quiescent cells. Of the other potential HSC niche components (13), the expression of Tie2 and JAG1 were
214 raised but not significantly in the quiescent cells (Figure 2A, Supplementary data table 1). The expression
215 of melanoma cell adhesion molecule (MCAM, CD146) and nestin were significantly lower in quiescent
216 compared to the non-quiescent cells. While the quiescent cells expressed putative prostate stem cell
217 markers, CD44, and integrins ⍺2/β1, there were no significant differences between expression levels in
218 these cells compared to the proliferating population (Figure 2B). Expression of a further prostate stem cell
219 marker, CD133, was very low in both populations (CT<35 cycles).

220

221 The presence of protein encoded by 3 genes that were differentially expressed between DiD retaining and

222 proliferating cells in the low density arrays, CXCR4, follistatin and MMP3 was assessed by

223 immunofluoresecent staining of cytospin preparations from mixed cultures (Figure 2 C). Comparisons from

224 multiple experiments showed that DiD positive cells expressed high levels of CXCR4 staining. However,

225 there were no correlations between the presence of the other antigens and the transcript levels of the genes

226 encoding these proteins or any associations with the quiescent phenotype Figure 2 C, D, E, F).

227

Inhibition of CXCR4 alters the association of tumour cells with bone surfaces

229 We were able to track tumour cells in vivo by pre-staining populations with DiD and examining tibias post-

230 mortem, by 2-photon microscopy. Animals injected with all three prostate cancer cell lines showed DiD

231 labeled cells present in bone, signals that were absent from naïve mice (Figure 3A). Cells arrived in the

232 tibia within 24h, accumulated during the first week and then declined slowly over the following weeks

233 (Figure 3B). However, DiD +ve quiescent cells were still detectable in bone at 6 weeks. Tumour growth

234 was monitored by bioluminescence as PC3-NW1 cells expressed luciferase. Growing lesions were

235 generally detected after 3-4 weeks post-injection. The positions of tumour cells relative to bone were

236 mapped and were shown to be in close proximity to bone (within 40   m) but there was a gradual but not

237 significant increase in the distance from bone structures with time (Figure 3C).

238

239 To test the functional involvement of CXCR4 signaling in the retention of tumour cells within bone, cohorts

240 of animals were treated with an agent that interferes with CXCR4 signaling (AMD3100) one week after

241 injection with tumour cells (schematic: Figure 3D). This resulted in a significant shift in the positioning of

242 tumour cells relative to bone surfaces (Figure 3E). There was no significant reduction in the total number

243 of tumour cells detected within bone (Figure 3F), suggesting that tumour cells were not mobilized back

244 into the circulation by this treatment.

245

The mitotically quiescent phenotype in vitro is more tumorigenic in vivo than proliferating cells.

247 We tested the hypothesis that the quiescent population, present in vitro was more tumorogenic in vivo. To

248 do this, 5×10^5 mitotically quiescent (DiD+) or proliferating (DiD- on sorting, restained with CM-Dil so

249 they could be tracked in vivo were injected (i.c.) into 6-week old animals to evaluate their tumourogenecity

250 (Figure 4A). Animals were culled between 6-10 weeks post-injection of tumor cells, depending on severity

251 of tumor burden. At this stage, both DiD+ and CM-Dil+ cells (sorted as DiD-) were present as single cells

252 within the tibias examined by 2-photon microscopy using channels that discriminated DiD/CM-DiI labeled

253 cells (Figure 4B). There were no DiD labeled cells detected amongst those labeled with CM-Dil. Neither

254 the FACS sorting nor CM-DiI staining affected the tumourogenicity of PC3-NW1 as injection of 10^5

255 unsorted cells or sorted CM-DiI restained cells produced high frequencies of growing tumours in skeleton

256 (>80%) as in previous studies. This confirms that dye staining and FACS treatment did not affect tumour

257 formation rates.

258

259 Injection of 5×10^3 DiD- cells formed skeletal lesions in only 15% of animals, with no long bone lesions.

260 Animals Injected with 5×10^3 DiD+ cells produced tumours in 55-60% of animals and tumors were observed

261 in long bone tumors at week 6 post injection via the IVIS system and further anatomical confirmation post

262 mortem (Figure 4C). Analyzed using the Living Imaging® In Vivo Imaging software, both the number of

263 tumours in bone per mouse and the total bone tumour burden (photon radiance) of each mouse, were both

264 statistically significantly higher in the group of mice injected with DiD+ cells (Figure 4D, 4E), further

265 confirming the higher tumourogenicity of quiescent cells in skeleton. Interestingly, there were no tumours

266 present in non-skeletal sites in animals injected with cells that retained DiD for 14 days in cell culture while

267 soft tissue tumours were seen in those that were injected with DiD –ve sorted populations.

268

269

Discussion

Two key findings have been demonstrated in these studies. Firstly we have shown that the widely used human prostate cancer cell lines PC3 and LNCaP and its variant C4 2B4 contain populations of cells that are slow growing/quiescent but not specifically stem like. These cells are present in cultures where the majority population grows rapidly under standard conditions. Secondly, when this population was isolated from PC3-NW1 cells, it was able to form skeletal tumors more frequently than the more, rapidly dividing population, when injected into immunosuppressed animals. Others have recently used this technology to identify slow-growing cell populations in the PC3 cell line (14) but have not characterized separate cell populations as we have done here.

We compared gene expression profiles of quiescent and proliferating populations using a low density array technology. The quiescent population in vitro expressed higher levels of CXCR4 and contained higher levels of this protein, measured by immunofluorescence, than non-quiescent cells. CXCR4 has been implicated in PC3 cell migration (10) and is required for the quiescence of HSC (15). The present study has identified CXCR4 as a marker of quiescent cells in a population with increased ability to form tumors in animals. Disruption of CXCR4 signaling using its antagonist AMD3100 did suggest that cells were induced to move away from bone surfaces and potentially away from osteoblast lineage cells a known source of the ligand SDF1 (CXCL12). This implies involvement of this signaling system in the homing process as suggested by others using these models (10) where this treatment was shown to result in tumour cells re-entering the circulation. We did not see any reduction of tumour numbers in bone in our study that would have been indicative of remobilization of tumor cells to the circulation nor did we see an increase in circulating tumor cells in treated animals.

While the expression of other genes in the selected arrays were increased, this did not appear to be reflected in increases in specific protein levels, apart from CXCR4. There may be a number of reasons for this. Firstly, there may be genuinely no increased protein production associated with the elevated transcript levels observed. Alternatively, we may not have chosen the correct time window to observe increased protein levels or the assays were not sensitive enough to detect differences. However, the relationship between elevated expression of some of the other genes and cell migration/metastasis may be still worth considering. Of the other genes that were significantly upregulated as measured by QRT-PCR in the quiescent cell population, MMP3 is linked to the expression of CXCR4. This protease has been shown to be elevated in the serum of patients with metastatic prostate cancer (16) and its inhibition by treatment of animals with TIMP3, suppressed the formation of PC3 tumors (17). Others have shown that MMP3

10

expression is induced by CXCR4 signaling (18). MMP2 has been shown to be present in patient bone biopsies and in PC3 xenografts where it has been shown to induce recruitment of osteoclasts/participate in the formation of lytic bone disease (19). Others have shown that experimentally induced expression V 6 integrin increased MMP2 production by PC3 cells and promoted osteolytic activity in vivo (20). The expression of fibronectin, a binding partner for V 6 integrin was also increased in the quiescent cells. Fibronectin is induced in EMT and has been associated with metastatic phenotype in breast cancer (21) as well as in prostate cancer cells (22) where overexpression of miR200b inhibited EMT, metastasis and downregulated fibronectin expression. Vitronectin has been associated with metastasis in breast cancer where binding of $\alpha V\beta 3$ integrin facilitated invasion under hypoxic conditions (23). Associations of vitronectin with this integrin have also been implicated as a driver of adhesion and invasion in prostate cancer (24). The present study would suggest that autologous production of ECM glycoproteins is a part of the quiescent, metastasis initiating phenotype. Similarly, tenascin C, which is produced by PC3 cells and expression elevated in the quiescent cells in our study, has been variably linked to reactive stroma in prostate cancer progression (25).

The present study suggested that the quiescent population in the PC3-NW1 cell line did not specifically share the full putative prostate stem cell phenotype (1). In particular, the quiescent cells did not express CD133, but did express high levels of integrin β1 and CD44. However there were no significant differences in the levels of expression of these markers between quiescent and non-quiescent cells. In contrast the expression of PSCA was elevated in the quiescent population. This protein is highly expressed in prostate cancer compared to normal tissues and has been associated with tumor progression (26, 27). We conclude that while the quiescent population carries some stem cell markers these do not uniquely identify this population. It is quiescence itself that is specifically associated with increased capacity to form metastatic lesions in xenograft models.

Taken together, the gene expression profiling data presented in this study suggests that the cells that are quiescent in vitro express higher levels of transcripts consistent with an invasive, metastatic phenotype. How and why this rare population is present or is generated in vitro remains to be discovered.

The in vivo studies clearly demonstrated that the quiescent cells isolated from cell cultures were more tumourogenic in initiating tumours in bone than rapidly dividing populations. This suggests that the quiescent population contains higher numbers of cells capable of surviving in the circulation, homing to the bone marrow and eventually being activated to form growing lesions.

337 Our studies suggest that mitotic quiescence, as defined by retention of the DiD dye for long periods, is in

338 itself a marker for increased ability to form metastases in experimental animals. These cells carry some of

339 the putative prostate cancer stem cell markers suggested by others but these are not exclusive to the

340 quiescent phenotype. The consistently increased expression of CXCR4 in the quiescent population would

341 enhance migration to bone for this cell type, which may, in part, provide an explanation for the increased

342 capacity of these cells to generate lesions in bone. The presence of increased levels of this protein in tumour

343 populations may be useful in predicting their capacity for migration and metastasis formation. In our

344 previous studies, we have highlighted problems in detecting CXCR4 in prostate cancer tissues (7). In

345 particular, we showed that the staining patterns reported were prone to artifact and that the overall frequency

346 of CXCR4 staining was low in prostate tissues. To date, there have been no definitive, properly validated

347 studies using primary prostate cancer tissue arrays with good clinical follow-up to test the hypothesis that

348 the presence of CXCR4 in subpopulations of cells in these tissues predicts the presence of occult metastases

349 in patients. Our studies and others (10) would suggest that this now needs to be given priority, especially

350 where patients are being diagnosed with early stage disease and for whom prognosis is currently not clearly

351 defined.

352

353 In conclusion, our study is the first to show that mitotic quiescence identifies cells with the highest capacity

354 to form bone metastases in prostate cancer models. This is counterintuitive in that it might be expected that

355 rapidly growing populations would be more capable of forming lesions. However our studies show that the

356 quiescent phenotype, with its consistent gene expression profile, in particular the production of CXCR4,

357 allows cells to survive and home to bone where mitotic quiescence persists until proliferation is initiated.

358

365

366 **References:**

367

368 1.   Collins, A. T., Berry, P. A., Hyde, C., Stower, M. J., and Maitland, N. J. (2005) Prospective
369   identification of tumorigenic prostate cancer stem cells. Cancer Res **65**, 10946-10951

370 2. Pellacani, D., Oldridge, E. E., Collins, A. T., and Maitland, N. J. (2013) Prominin-1 (CD133)
371   Expression in the Prostate and Prostate Cancer: A Marker for Quiescent Stem Cells. Adv Exp Med
372   Biol **777**, 167-184
373 3. Sheng, X., Li, Z., Wang, D. L., Li, W. B., Luo, Z., Chen, K. H., Cao, J. J., Yu, C., and Liu, W. J.
374   (2013) Isolation and enrichment of PC-3 prostate cancer stem-like cells using MACS and serum-
375   free medium. Oncol Lett **5**, 787-792
376 4. Williamson, S. C., Hepburn, A. C., Wilson, L., Coffey, K., Ryan-Munden, C. A., Pal, D., Leung,
377   H. Y., Robson, C. N., and Heer, R. (2012) Human alpha(2)beta(1)(HI) CD133(+VE) epithelial
378   prostate stem cells express low levels of active androgen receptor. PLoS One **7**, e48944
379 5. Guzman-Ramirez, N., Voller, M., Wetterwald, A., Germann, M., Cross, N. A., Rentsch, C. A.,
380   Schalken, J., Thalmann, G. N., and Cecchini, M. G. (2009) In vitro propagation and
381   characterization of neoplastic stem/progenitor-like cells from human prostate cancer tissue.
382   Prostate **69**, 1683-1693
383 6. Colombel, M., Eaton, C. L., Hamdy, F., Ricci, E., van der Pluijm, G., Cecchini, M., Mege-
384   Lechevallier, F., Clezardin, P., and Thalmann, G. (2012) Increased expression of putative cancer
385   stem cell markers in primary prostate cancer is associated with progression of bone metastases.
386   Prostate **72**, 713-720
387 7. Eaton, C. L., Colombel, M., van der Pluijm, G., Cecchini, M., Wetterwald, A., Lippitt, J.,
388   Rehman, I., Hamdy, F., and Thalman, G. (2010) Evaluation of the frequency of putative prostate
389   cancer stem cells in primary and metastatic prostate cancer. Prostate **70**, 875-882
390 8. Germann, M., Wetterwald, A., Guzman-Ramirez, N., van der Pluijm, G., Culig, Z., Cecchini, M.
391   G., Williams, E. D., and Thalmann, G. N. (2012) Stem-like cells with luminal progenitor
392   phenotype survive castration in human prostate cancer. Stem Cells **30**, 1076-1086
393 9. Polson, E. S., Lewis, J. L., Celik, H., Mann, V. M., Stower, M. J., Simms, M. S., Rodrigues, G.,
394   Collins, A. T., and Maitland, N. J. (2013) Monoallelic expression of TMPRSS2/ERG in prostate
395   cancer stem cells. Nat Commun **4**, 1623
396 10. Shiozawa, Y., Pedersen, E. A., Havens, A. M., Jung, Y., Mishra, A., Joseph, J., Kim, J. K., Patel,
397   L. R., Ying, C., Ziegler, A. M., Pienta, M. J., Song, J., Wang, J., Loberg, R. D., Krebsbach, P. H.,
398   Pienta, K. J., and Taichman, R. S. (2011) Human prostate cancer metastases target the
399   hematopoietic stem cell niche to establish footholds in mouse bone marrow. J Clin Invest **121**,
400   1298-1312
401 11. Pece, S., Tosoni, D., Confalonieri, S., Mazzarol, G., Vecchi, M., Ronzoni, S., Bernard, L., Viale,
402   G., Pelicci, P. G., and Di Fiore, P. P. (2010) Biological and molecular heterogeneity of breast
403   cancers correlates with their cancer stem cell content. Cell **140**, 62-73
404 12. Wang, N., Docherty, F. E., Brown, H. K., Reeves, K. J., Fowles, A. C., Ottewell, P. D., Dear, T.
405   N., Holen, I., Croucher, P. I., and Eaton, C. L. (2014) Prostate cancer cells preferentially home to
406   osteoblast-rich areas in the early stages of bone metastasis - evidence from in vivo models. J Bone
407   Miner Res
408 13. Arai, F., Hirao, A., Ohmura, M., Sato, H., Matsuoka, S., Takubo, K., Ito, K., Koh, G. Y., and
409   Suda, T. (2004) Tie2/angiopoietin-1 signaling regulates hematopoietic stem cell quiescence in the
410   bone marrow niche. Cell **118**, 149-161
411 14. Yumoto, K., Berry, J. E., Taichman, R. S., and Shiozawa, Y. (2014) A novel method for
412   monitoring tumor proliferation in vivo using fluorescent dye DiD. Cytometry A **85**, 548-555
413 15. Nie, Y., Han, Y. C., and Zou, Y. R. (2008) CXCR4 is required for the quiescence of primitive
414   hematopoietic cells. J Exp Med **205**, 777-783
415 16. Jung, K., Nowak, L., Lein, M., Priem, F., Schnorr, D., and Loening, S. A. (1997) Matrix
416   metalloproteinases 1 and 3, tissue inhibitor of metalloproteinase-1 and the complex of
417   metalloproteinase-1/tissue inhibitor in plasma of patients with prostate cancer. Int J Cancer **74**,
418   220-223

419   17.   Zhang, L., Zhao, L., Zhao, D., Lin, G., Guo, B., Li, Y., Liang, Z., Zhao, X. J., and Fang, X. (2010)
420   Inhibition of tumor growth and induction of apoptosis in prostate cancer cell lines by
421   overexpression of tissue inhibitor of matrix metalloproteinase-3. Cancer Gene Ther **17**, 171-179
422   18.   Singh, S., Singh, U. P., Grizzle, W. E., and Lillard, J. W., Jr. (2004) CXCL12-CXCR4
423   interactions modulate prostate cancer cell migration, metalloproteinase expression and invasion.
424   Lab Invest **84**, 1666-1676
425   19.   Nemeth, J. A., Yousif, R., Herzog, M., Che, M., Upadhyay, J., Shekarriz, B., Bhagat, S., Mullins,
426   C., Fridman, R., and Cher, M. L. (2002) Matrix metalloproteinase activity, bone matrix turnover,
427   and tumor cell proliferation in prostate cancer bone metastasis. J Natl Cancer Inst **94**, 17-25
428   20.   Dutta, A., Li, J., Lu, H., Akech, J., Pratap, J., Wang, T., Zerlanko, B. J., FitzGerald, T. J., Jiang,
429   Z., Birbe, R., Wixted, J., Violette, S. M., Stein, J. L., Stein, G. S., Lian, J. B., and Languino, L. R.
430   (2014) Integrin alphavbeta6 promotes an osteolytic program in cancer cells by upregulating
431   MMP2. Cancer Res **74**, 1598-1608
432   21.   Nutter, F., Holen, I., Brown, H. K., Cross, S. S., Evans, C. A., Walker, M., Coleman, R. E.,
433   Westbrook, J. A., Selby, P. J., Brown, J. E., and Ottewell, P. D. (2014) Different molecular
434   profiles are associated with breast cancer cell homing compared with colonisation of bone:
435   evidence using a novel bone-seeking cell line. Endocr Relat Cancer **21**, 327-341
436   22.   Williams, L. V., Veliceasa, D., Vinokour, E., and Volpert, O. V. (2013) miR-200b inhibits
437   prostate cancer EMT, growth and metastasis. PLoS One **8**, e83991
438   23.   Pola, C., Formenti, S. C., and Schneider, R. J. (2013) Vitronectin-alphavbeta3 integrin
439   engagement directs hypoxia-resistant mTOR activity and sustained protein synthesis linked to
440   invasion by breast cancer cells. Cancer Res **73**, 4571-4578
441   24.   Cooper, C. R., Chay, C. H., and Pienta, K. J. (2002) The role of alpha(v)beta(3) in prostate cancer
442   progression. Neoplasia **4**, 191-194
443   25.   Reinertsen, T., Halgunset, J., Viset, T., Flatberg, A., Haugsmoen, L. L., and Skogseth, H. (2012)
444   Gene expressional changes in prostate fibroblasts from cancerous tissue. APMIS **120**, 558-571
445   26.   Reiter, R. E., Gu, Z., Watabe, T., Thomas, G., Szigeti, K., Davis, E., Wahl, M., Nisitani, S.,
446   Yamashiro, J., Le Beau, M. M., Loda, M., and Witte, O. N. (1998) Prostate stem cell antigen: a
447   cell surface marker overexpressed in prostate cancer. Proc Natl Acad Sci U S A **95**, 1735-1740
448   27.   Gu, Z., Thomas, G., Yamashiro, J., Shintaku, I. P., Dorey, F., Raitano, A., Witte, O. N., Said, J.
449   W., Loda, M., and Reiter, R. E. (2000) Prostate stem cell antigen (PSCA) expression increases
450   with high gleason score, advanced stage and bone metastasis in prostate cancer. Oncogene **19**,
451   1288-1296

452

453

454   **Figure Legends:**

455

456   **Figure 1: Defining the mitotically quiescent population in prostate cancer cell lines.**

457

458   A) Analysis of the retention of DiD labeling in cultures of PC3-NW1 cells in the presence and

459   absence of mitomycin C for up to 3 weeks by flow cytometry. (n=3, **** p<0.0001, t test).

460   B) A representative dot plot of flow cytometry gating shows distinct population of prostate cancer

461   cells which maintain DiD labeling after 14 days of culture.

462   C) Dye content (% DiD+ve) of PC3-NW1, LNCap and C42B4 stained with DiD were followed and

463   analyzed for 14 days by flow cytometry. (n=3).

14

D) The effects of DiD labeling on proliferation over standard growth curves up to 12 days in culture. (n=3)

E) Cells that retained DiD for 14 days were isolated by FACS and re-cultured at clonal density. Immunofluorescence microscopy was used to visualize DiD +ve cells at day 2, 6 and 10 post-seeding. Scale bar = 50µm.

F) Immunofluorescent image of mixed population with dye retaining cells (DiD+, Red) and proliferating cells (DiD-) were immunostained with mouse anti-human Ki-67 antibody (Green) and counterstained with DAPI (Blue). Scale bar = 50µm.

G) Comparison of the percentage of Ki67 positivity between DiD+ and DiD- populations by flow cytometry analysis. (n=3, *** $p<0.001$, t test).

Figure 2: Characterization of quiescent vs non-quiescent cells

A) Fold differences in expression of connective tissue proteins, markers of EMT, and HSC niche molecules, compared between quiescent vs non-quiescent cells.   CT was relative to the housekeeping gene (GAPDH) measured by QRT-PCR in low-density arrays. (n=3, significant changes = fold differences >2 or < 0.5)

B) Fold differences in expression of putative cancer stem cell markers, compared between quiescent vs non-quiescent cells.   CT was relative to the housekeeping gene (GAPDH) measured by QRT-PCR in low-density arrays. (n=3, significant changes = fold differences >2 or < 0.5) ITGA2 : integrin a2, ITGB1: integrin b1

C) Immunofluorescence staining showing that DiD labeled, quiescent PC3-NW1 cells (red) correlated with higher expression of CXCR4 protein (PE+, Green) but neither FST (Green) nor MMP3 (Green), following 14 days of culture after the initial DiD staining.

D) The immunofluorescence staining intensity of CXCR4,

E) FST, and

F) MMP3 were quantified with ImageJ software and compared between DiD+ and DiD- populations. (Scale bar = 50µm. n=3, * $p<0.05$, ** $p<0.01$, paired t test)

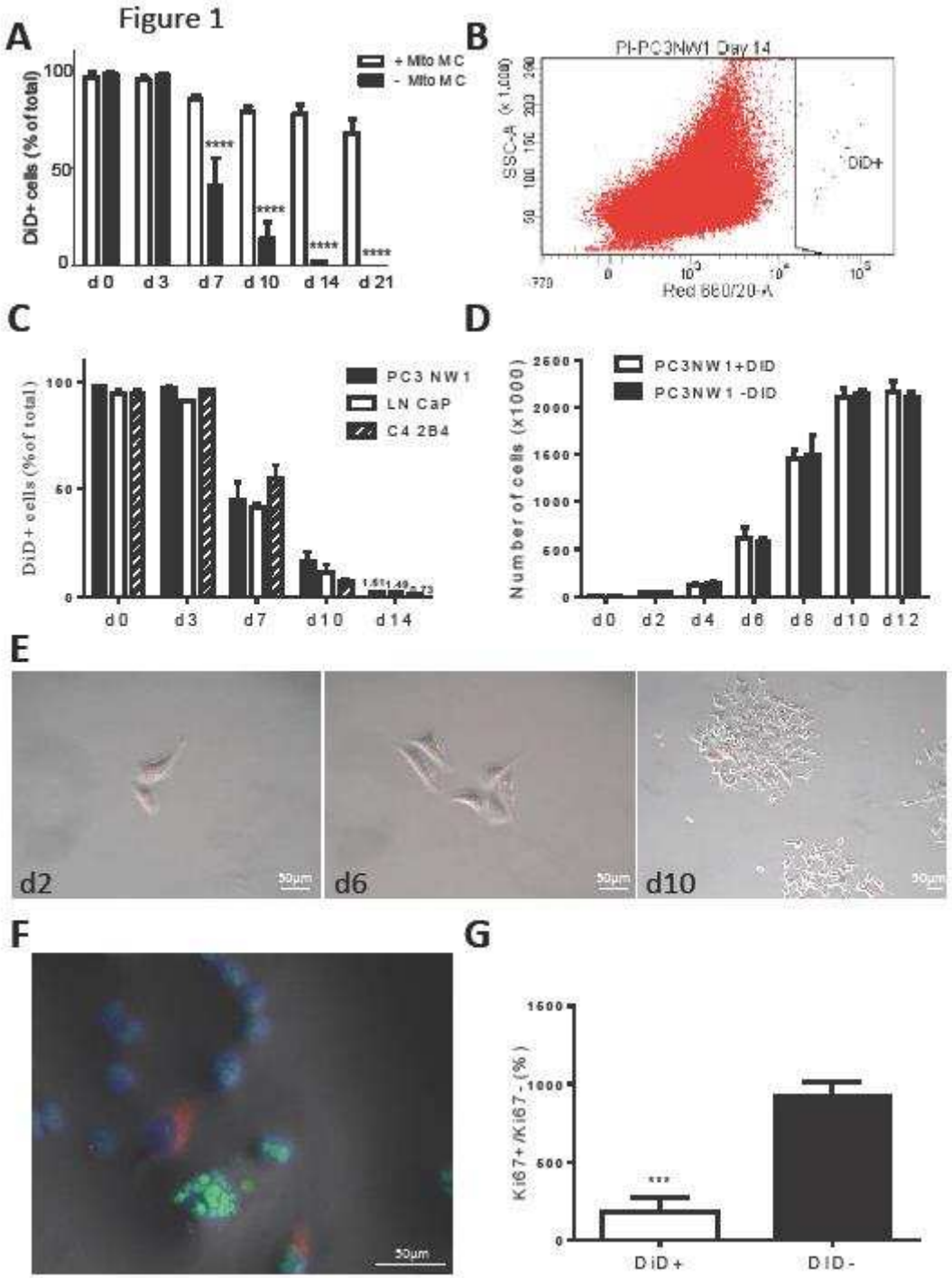**Figure 3. Disruption of CXCR4 interactions induces a shift in tumour cell position in bone.**

A) Two-photon scans of tibias from naïve mice and mice injected (intracardiac) with DiD labeled PC3-NW1, C4 2B4, and LNCaP cells, 7 days post injection. DiD labeled cells indicated (yellow arrows)
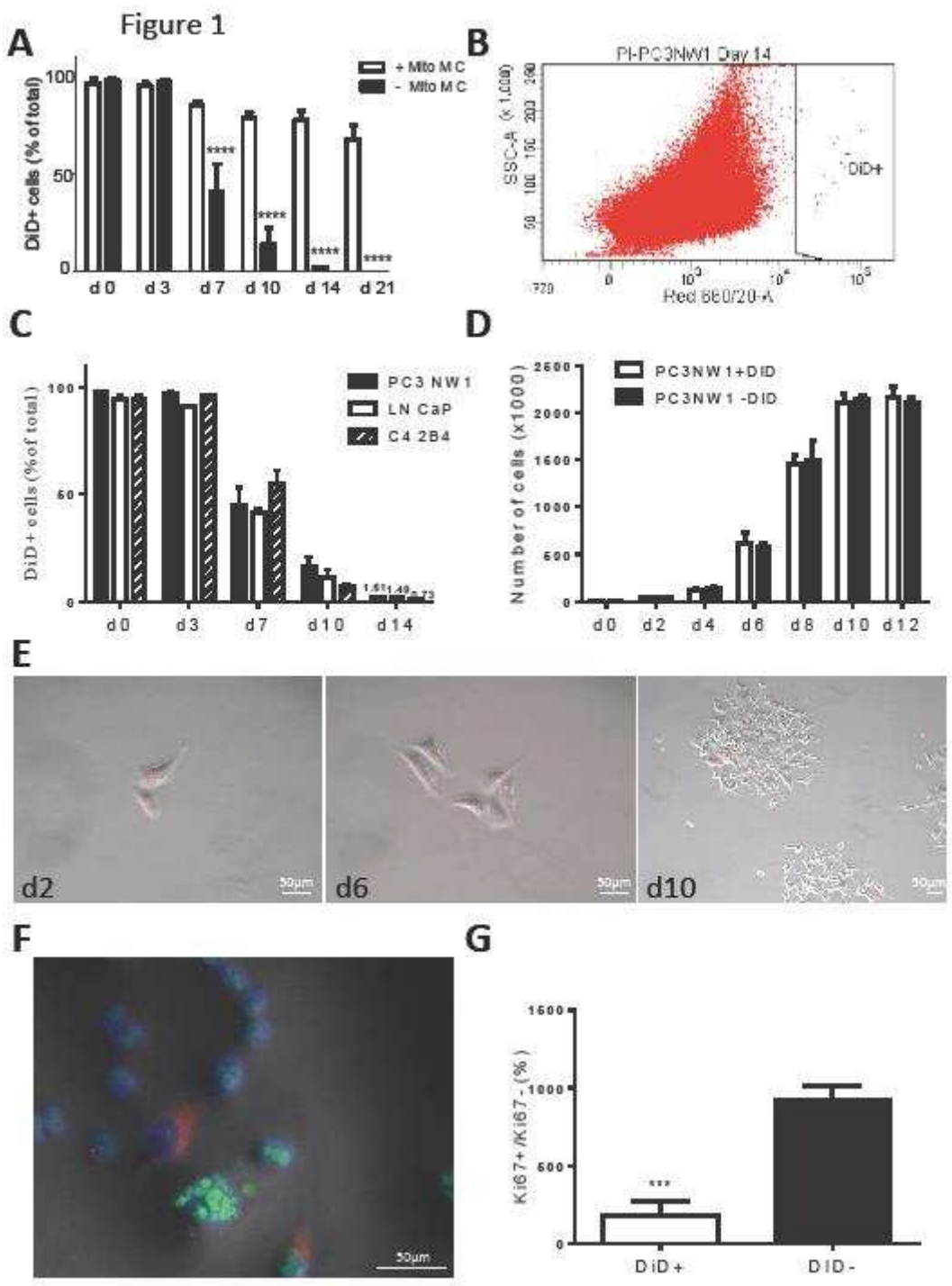
497   B) Frequency of DiD labeled tumor cells per mm^3 bone marrow detected by 2-photon microscopy in
498   tibias of a cohort of mice injected (intracardiac) with PC3-NW1 cells over a 6 weeks of time post
499   injection (n > 6, ** $p<0.01$, one-way ANOVA with post Tukey test).

500   C) The position of tumour cells relative to bone surfaces over time mapped using the Volocity 3D
501   Image Analysis software. (n > 6).

502   D) Schematic outline of the procedure used to inhibit CXCR4 and evaluate the association of tumour
503   cells and bone: 6-week old athymic mice were injected (intracardiac) with DiD labeled PC3-NW1
504   and daily treatment of CXCR4 antagonist (AMD3100) were started 7 days post injection for five
505   consecutive days. The mice were then euthanized 24hr later for 2-photon microscopy analysis.

506   E) The distance from tumour cells to the nearest bone surface, and

507   F) The number of DiD labelled tumour cell per mm^3 bone marrow were compared between the
508   AMD3100 treated and control animals. (n=8, ** $p<0.01$, t test).

509

510 **Figure 4: Assessment of the growth and tumor initiating capacity of mitotically quiescent prostate**
511 **cancer cells in vivo.**

512

513   A) Schematic outline of the procedure used to isolate and evaluate the tumorogenicity of mitotically
514   quiescent and dividing cells in vivo: PC3-NW1 cells were stained with DiD and cultured
515   continuously in standard medium for 14 days. DiD retaining (DiD+) and non-retaining DiD- cells
516   were FACS sorted and DiD- cells were restained with CM-Dil. Different populations were then
517   injected intracardiac into athymic mice including mitotically quiescent (DiD+, $5x10^3$
518   cells/mouse), non-quiescent populations (DiD-, $5x10^3$ cells/mouse) and the whole, mock-sorted
519   population ($1x10^5$ cells/mouse).

520   B) DiD (upper panel) or CM-DiI (DiD-, lower panel) labeled tumor cells were visualized in tibias by
521   two-photon microscopy (arrows), 6 weeks post injection.

522   C) The tumourogenecity in the skeleton especially in long bone were visualized by bioluminescence
523   for 6 weeks post injection using IVIS system and compared between groups injected with DiD+
524   cells (n=15) and DiD- cells (n=15).

525   D) The number of tumours per mouse, and

526   E) Tumour burden (photon radiance) was analyzed and compared between the two groups using the
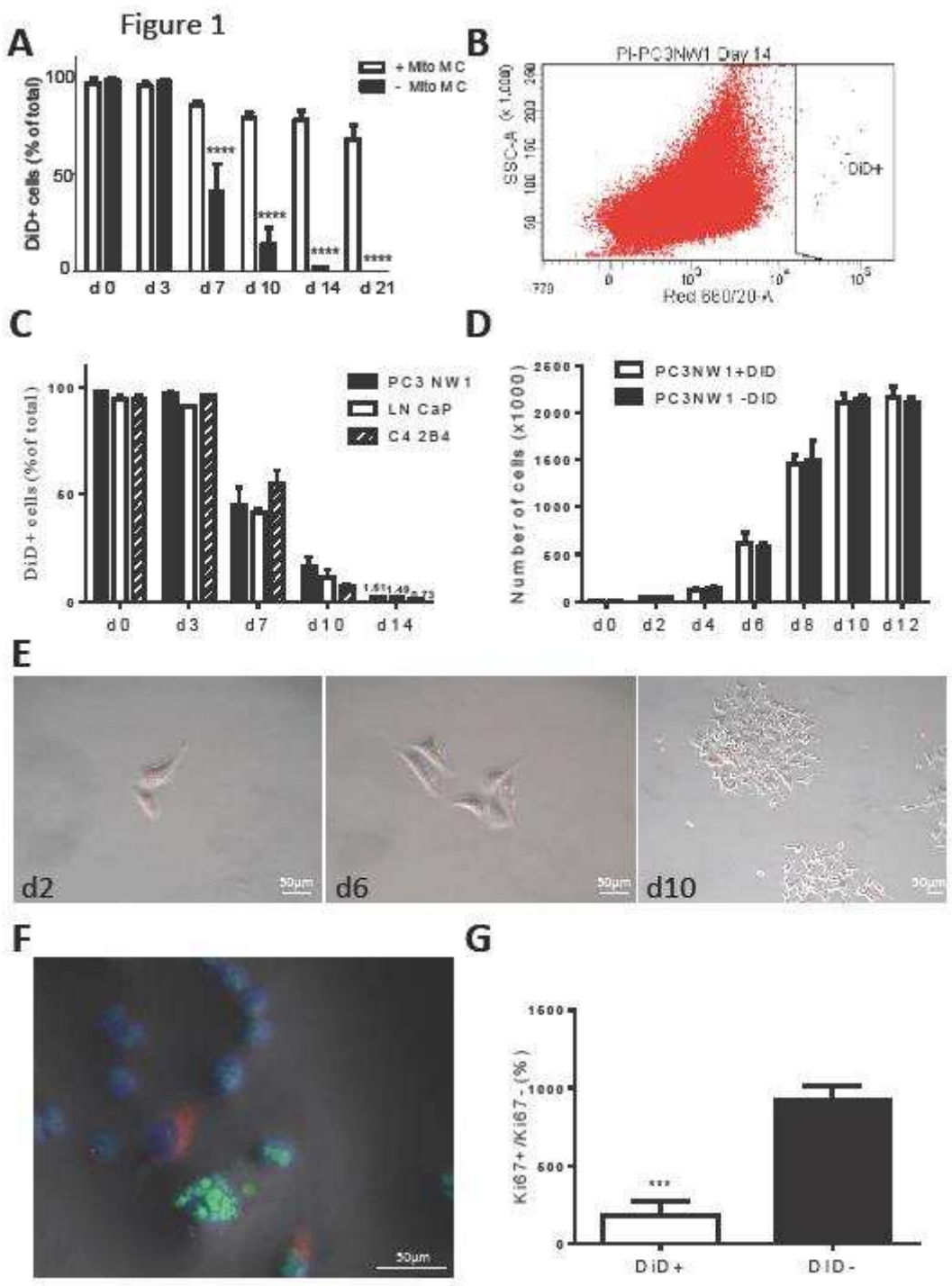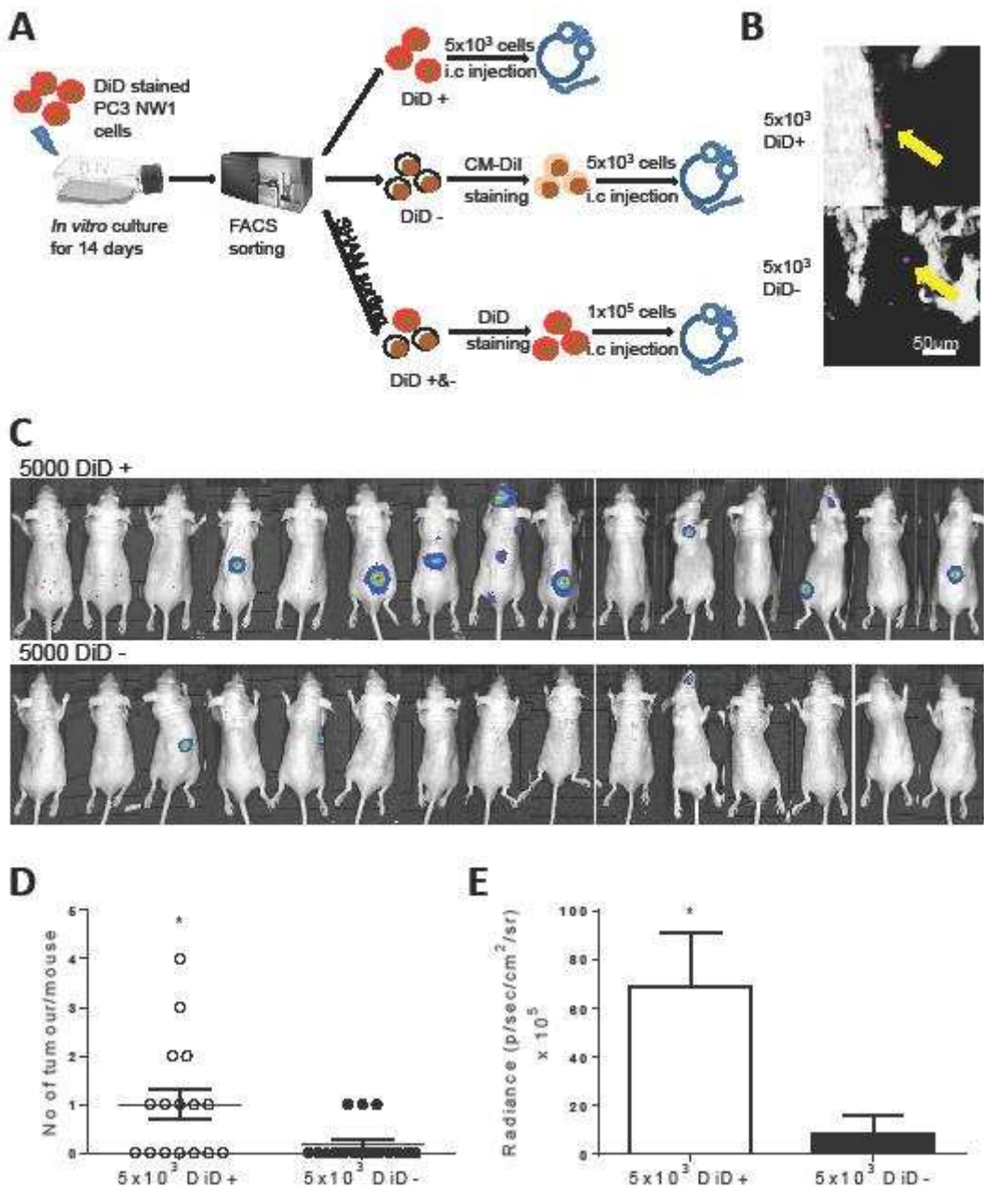527   Living Image software. (n=15, * $p<0.05$, t test).

528

529   Figure 1

530
531

17

532   Figure 2

533
534

18

535   Figure 3

536
537

538   Figure 4

Figure 4

539
540

Table 1 (Eaton)

Gene Abbreviation	DiD+ (ΔCt)	DiD-(ΔCt)	P value	Gene Abbreviation	DiD+(ΔCt)	DiD-(ΔCt)	P value
ACPP	9.90 ± 0.288	9.94 ± 0.179	0.499	KLK3	ND	ND	
ACTA2	15.40 ± 0.451	15.85 ± 0.236	0.424	KRT18	11.11 ± 0.315	11.06 ± 0.172	0.906
ADAMTS1	9.61 ± 0.443	10.50 ± 0.188	0.187	KRT5	ND	ND	
ADM2	12.27 ± 0.448	12.65 ± 0.318	0.529	KRT8	16.44 ± 0.357	16.92 ± 0.492	0.472
AKT1	5.85 ± 0.379	6.02 ± 0.196	0.717	LDHA	2.88 ± 0.295	3.22 ± 0.166	0.366
ALDH7A1	8.69 ± 0.399	8.17 ± 0.160	0.298	LDHB	5.01 ± 0.457	4.04 ± 0.194	0.124
ALPL	19.76 ± 1.534	17.70 ± 0.435	0.266	MATN2	9.09 ± 0.343	10.81 ± 0.282	0.018
ANGPT1	15.36 ± 0.471	15.22 ± 0.362	0.815	MCAM	12.21 ± 0.369	10.91 ± 0.177	0.034
ANXA2	3.27 ± 0.408	3.87 ± 0.257	0.281	MMP2	16.29 ± 0.348	17.63 ± 0.320	0.047
AR	16.59 ± 0.519	17.00 ± 0.357	0.545	MMP3	13.39 ± 0.415	18.63 ± 0.754	0.004
AXL	10.14 ± 0.331	10.87 ± 0.210	0.138	MUC1	11.93 ± 0.293	12.48 ± 0.336	0.290
BGLAP	17.37 ± 0.570	17.09 ± 0.205	0.658	NANOG	11.93 ± 0.290	12.03 ± 0.853	0.919
BMI1	4.66 ± 0.335	5.06 ± 0.195	0.356	NES	9.47 ± 0.386	8.31 ± 0.201	0.056
BMP2	7.53 ± 0.350	8.33 ± 0.213	0.113	NOG	11.09 ± 0.467	11.05 ± 0.185	0.932
BMP6	7.96 ± 0.367	7.62 ± 0.163	0.061	NOTCH1	8.99 ± 0.289	8.57 ± 0.188	0.296
CD24	3.13 ± 0.320	4.04 ± 0.184	0.069	NR3C1	12.50 ± 0.397	13.16 ± 0.164	0.200
CD34	19.65 ± 1.465	21.51 ± 1.097	0.442	OCLN	8.15 ± 0.328	8.05 ± 0.207	0.818
CD38	13.88 ± 0.299	13.79 ± 0.221	0.826	PGR	18.60 ± 0.537	19.35 ± 1.315	0.627
CD44	4.66 ± 0.341	5.13 ± 0.161	0.283	POU5F1	11.94 ± 0.290	11.59 ± 0.674	0.663
CDH1	5.95 ± 0.293	6.29 ± 0.176	0.371	PROM1	ND	ND	
CDH2	6.33 ± 0.305	6.53 ± 0.410	0.717	PSCA	15.58 ± 0.378	18.61 ± 0.336	0.004
CDH7	11.34 ± 0.403	11.49 ± 0.358	0.799	PTEN	ND	ND	
CLDN4	6.77 ± 0.310	7.00 ± 0.192	0.566	RHOB	8.93 ± 0.311	8.62 ± 0.241	0.472
COL1A1	14.15 ± 0.400	16.52 ± 0.648	0.036	RUNX2	11.29 ± 0.422	11.13 ± 0.317	0.773
COX2	ND	ND		S100A4	7.51 ± 0.444	7.46 ± 0.187	0.924
CXCL1	11.00 ± 0.423	14.15 ± 0.172	0.002	SDC1	7.24 ± 0.475	7.43 ± 0.265	0.748
CXCL12	21.53 ± 1.018	21.68 ± 1.55	0.940	SHH	17.93 ± 0.514	20.81 ± 1.579	0.158
CXCL16	8.94 ± 0.293	8.81 ± 0.189	0.719	SOX2	12.57 ± 0.373	12.47 ± 0.338	0.859
CXCR4	7.58 ± 0.487	9.36 ± 0.462	0.057	SPARC	5.68 ± 0.390	5.80 ± 0.237	0.807
CXCR6	ND	ND		SPP1	ND	ND	
CXCR7	11.60 ± 0.418	12.27 ± 0.174	0.213	TEK	16.19 ± 0.421	17.25 ± 0.663	0.250
DKK1	2.97 ± 0.294	3.93 ± 0.269	0.072	TERT	13.07 ± 0.333	12.36 ± 0.381	0.231
DSP	9.95 ± 0.340	10.47 ± 0.353	0.344	TGFB1	5.69 ± 0.419	5.52 ± 0.335	0.759
ERG	19.89 ± 1.510	20.92 ± 1.500	0.655	TGFBR1	8.15 ± 0.345	8.00 ± 0.219	0.734
ESR1	17.23 ± 0.478	18.52 ± 0.372	0.100	TJP1	8.01 ± 0.287	8.10 ± 0.164	0.800
ESR2	14.71 ± 0.362	14.57 ± 0.241	0.768	TMPRSS2-ERGfusion	ND	ND	
FGF2	9.96 ± 0.289	10.80 ± 0.192	0.074				
FGF8	16.03 ± 0.840	15.57 ± 0.740	0.700	TMPRSS2	13.74 ± 0.321	15.60 ± 0.542	0.042
FN1	7.01 ± 0.287	9.98 ± 0.184	0.001	TNC	7.76 ± 0.315	9.06 ± 0.177	0.023
FST	7.21 ± 0.430	9.40 ± 0.392	0.020	TNFRSF11A	13.54 ± 0.652	12.63 ± 0.361	0.288
GAS6	18.52 ± 1.432	22.22 ± 0.922	0.096	TNFRSF11B	14.00 ± 0.403	13.98 ± 0.291	0.974
ITGA2	5.99 ± 0.374	6.91 ± 0.221	0.101	TNFSF11	ND	ND	
ITGA4	ND	ND		TP63	12.37 ± 0.430	9.50 ± 4.500	0.560
ITGB1	3.83 ± 0.332	4.47 ± 0.600	0.406	VIM	1.70 ± 0.417	1.74 ± 0.281	0.935
JAG1	7.26 ± 0.341	7.84 ± 0.248	0.243	VTN	16.58 ± 0.461	21.20 ± 1.293	0.028
KIT	ND	ND					

541
542

Table 2 (Eaton)

Gene Abbreviation	Gene Name	Gene Abbreviation	Gene Name
ACPP	Acid Phosphatase, Prostate	KIT	V-Kit Hardy-Zuckerman 4 Feline Sarcoma Viral Oncogene Homolog
ACTA2	Actin, alpha 2	KLK3	Kallikrein-Related Peptidase 3
ADAMTS1	Metallopeptidase With Thrombospondin Type 1 Motif	KRT18	Keratin 18
ADM2	Adrenomedullin 2	KRT5	Keratin 5
AKT1	V-akt murine thymoma viral oncogene homolog 1	KRT8	Keratin 8
ALDH7A1	Aldehyde dehydrogenase 7 family, member A1	LDHA	Lactate dehydrogenase A
ALPL	Alkaline phosphatase	LDHB	Lactate dehydrogenase B
ANGPT1	Angiopoietin 1	MATN2	Matrilin 2
ANXA2	Annexin A2	MCAM	Melanoma cell adhesion molecule (CD146)
AR	Androgen receptor	MMP2	Matrix metalloproteinase-2
AXL	AXL Receptor Tyrosine Kinase	MMP3	Matrix metalloproteinase-3
BGLAP	Bone Gamma-Carboxyglutamate (Gla) Protein	MUC1	Mucin 1
BMI1	B lymphoma Mo-MLV insertion region 1 homolog1	NANOG	Nanog Homeobox
BMP2	Bone Morphogenetic Protein 2	NES	Nestin
BMP6	Bone Morphogenetic Protein 6	NOG	Noggin
BMP7	Bone Morphogenetic Protein 7	NOTCH1	NOTCH1
		NR3C1	Nuclear Receptor Subfamily 3, Group C, Member 1 (NR3C1)
CD24	Cluster of differentiation 24		
CD34	Cluster of differentiation 34	OCLN	Occludin
CD38	Cluster of differentiation 38	PGR	Progesterone receptor
CD44	Cluster of differentiation 44	POU5F1	POU Class 5 Homeobox 1(OCT4)
CDH1	E-cadherin	PROM1	Prominin 1(CD133)
CDH2	N-Cadherin	PSCA	Prostate stem cell antigen
CDH7	Cadherin 7, Type 2	PTEN	Phosphatase and tensin homolog
CLDN4	Claudin 4	RHOB	Ras Homolog Family Member B
COL1A1	Collagen, type I, alpha 1	RUNX2	Runt-Related Transcription Factor 2
COX2	Mitochondrially Encoded Cytochrome C Oxidase II	S100A4	Fibroblast-Specific Protein-1
CXCL1	Chemokine (C-X-C Motif) Ligand 1	SDC1	Syndecan 1
CXCL12	Chemokine (C-X-C Motif) Ligand 12	SHH	Sonic hedgehog
CXCL16	Chemokine (C-X-C Motif) Ligand 16	SOX2	SRY (Sex Determining Region Y)-Box 2
CXCR4	Chemokine (C-X-C Motif) Receptor 4	SPARC	Osteonectin
CXCR6	Chemokine (C-X-C Motif) Receptor 6	SPP1	Osteopontin
CXCR7	Chemokine (C-X-C Motif) Receptor 7	TEK	TEK Tyrosine Kinase, Endothelial
DKK1	Dickkopf WNT Signaling Pathway Inhibitor 1	TERT	Telomerase reverse transcriptase
DSP	Desmoplakin	TGFB1	Transforming Growth Factor, Beta 1
ERG	V-Ets Avian Erythroblastosis Virus E26 Oncogene Homolog	TGFBR1	Transforming Growth Factor, Beta Receptor 1
ESR1	Estrogen Receptor 1	TJP1	Tight Junction Protein 1
ESR2	Estrogen Receptor 2	TMPRSS2-ERG	TMPRSS2-ERGfusion
FGF2	Fibroblast growth factor 2		
FGF8	Fibroblast growth factor 8	TMPRSS2	Transmembrane Protease, Serine 2
FN1	Fibronectin	TNC	Tenascin C
		TNFRSF11A	Tumor Necrosis Factor Receptor Superfamily, Member 11a, NFKB Activator(RANK)
FST	Follistatin		
GAS6	Growth arrest-specific 6	TNFRSF11B	Osteoprotegerin
		TNFSF11	Tumor Necrosis Factor (Ligand) Superfamily, Member 11(RANKL)
ITGA2	Integrin, Alpha 2		
ITGA4	Integrin, Alpha 4	TP63	Tumour Protein P63
ITGB1	Integrin, Beta 1	VIM	Vimentin
JAG1	Jagged 1	VTN	Vitronectin

543
544

22

Supplementary Data Legends:
Table 1
Complete list of all genes analyzed by QRT-PCR in low-density arrays. Data presented is combined from 3 independent experiments. ΔCT values for differences between DiD+ and DiD- cells are presented along with p values (t test).

Table 2
Complete list of genes evaluated by QRT-PCR on low-density arrays with abbreviations used.

545